RESEARCH PAPER

MAJORITY FILTER FOR ENHANCING PIXEL-BASED RANDOM FOREST LAND COVER CLASSIFICATION IN SUKAJAYA DISTRICT, BOGOR REGENCY

Fathan Aldi Rivai[1*], Boedi Tjahjono[1], Khursatul Munibah[1], Adenan Yandra Nofrizal[2]

[1]Department of Soil Science and Land Resources, Faculty of Agriculture, IPB University, Dramaga Main Road, 16680, Bogor Regency, Indonesia

[2]Department of Applied Geoinformatics and Cartography, Faculty of Science, Charles University, Albertov 6, 128 43, Prague, Czech Republic

Received: July 29th 2025 / Accepted: November 12nd 2025 / Published: December 31st 2025

***Corresponding author:** r.fathan.aldi@gmail.com

https://doi.org/10.24057/2071-9388-2025-4183

ABSTRACT. High-quality land cover data are essential for environmental policy, spatial planning, and ecosystem monitoring. However, pixel-based classification methods, while widely used due to their practicality, often suffer from salt-and-pepper noise, which undermines map reliability. This study aimed to integrate Random Forest (RF) classification and majority filtering to enhance the quality of land cover mapping in Sukajaya District, Bogor Regency. RF was applied to Sentinel-2 image data with varying numbers of trees (ntree) to determine the optimal model performance. Subsequently, majority filtering was applied to each classification result to reduce noise and improve spatial coherence. The evaluation employed multiple accuracy metrics, including User's Accuracy (UA), Producer's Accuracy (PA), F1-Score, Overall Accuracy (OA), and Kappa Coefficient (KC). Comprehensive accuracy increased with the ntree until reaching an optimal point. Beyond this point, additional ntree resulted in diminishing returns. Applying majority filtering as a post-processing procedure led to further improvements in classification accuracy. While majority filtering can reduce classification noise and improve the visual quality of land cover maps, it also carries the risk of removing small, accurately classified land cover patches. This consequence is rarely discussed in similar studies. These findings highlight the importance of integrating pixel-based machine learning classification with majority filtering in land cover classification workflows, while emphasising a trade-off that tends to favour visual accuracy over the preservation of spatial detail.

KEYWORDS: Diminishing return, Majority filter, Pixel-based classification, Random Forest, Salt-and-pepper noise

CITATION: Rivai F. A., Tjahjono B., Munibah K., Nofrizal A. Y. (2025). Majority Filter For Enhancing Pixel-Based Random Forest Land Cover Classification In Sukajaya District, Bogor Regency. Geography, Environment, Sustainability, 4 (18), 171-182
https://doi.org/10.24057/2071-9388-2025-4183

Conflict of interests: The authors reported no potential conflict of interests.

INTRODUCTION

Land cover is a critical aspect of the Earth's surface and a key consideration in territorial policymaking. It reflects the spatial distribution of ecosystems and provides quantitative indications of land-based service potentials (Anthony et al., 2024). This information supports evidence-based planning by offering an objective foundation for assessing environmental conditions (Aslam et al., 2024). When analysed temporally, land cover data can be used to identify landscape dynamics (Qacami et al., 2023). Variations in land cover types influence carbon stock differences, making it a vital component in emissions accounting (Solomon et al., 2018; Zhu et al., 2022). This data also plays a crucial role in hydrological process modelling (Mensah et al., 2022) and habitat suitability assessments for biodiversity conservation (Edosa and Erena, 2024). Collectively, these applications highlight the strategic importance of land cover in supporting conservation policies and adaptation to environmental change.

Land cover mapping using field surveys demands considerable time and resources. The development of geographic information systems, remote sensing technologies, and machine learning algorithms has increased the efficiency of this process. Random Forest (RF) is one of the most commonly used algorithms for land cover classification. This algorithm uses a bootstrap aggregation (bagging) method by building multiple decision trees from random subsets of the training data (Altman and Krzywinski, 2017; Rivai et al., 2023). At each node, RF randomly chooses a subset of features to improve model diversity (Ibrahim, 2023). It is particularly effective at managing imbalanced training data (Chahal et al., 2024), which makes it highly suitable for land cover classification tasks. In these tasks, training data across different classes are usually uneven, especially when the proportions of land cover are very uneven.

RF is a reliable algorithm for land cover classification, with the number of trees (ntree) being its most critical hyperparameter. RF is widely used in pixel-based land cover classification due to its ability to deliver high accuracy with relatively efficient computational performance. This approach is considered more practical than object-based methods, which require complex and computationally

intensive segmentation steps (Ye et al., 2023; Behera et al., 2024). Consequently, pixel-based classification remains a common approach for generating land cover maps. However, pixel-based classification results often suffer from salt-and-pepper noise. This refers to pixels that are classified differently from their surrounding areas (Ebrahimy et al., 2021; El-Deen Taha and Mandouh, 2024; Fu et al., 2017). This issue is frequently overlooked in land cover classification studies. The focus is typically placed on improving overall accuracy without adequately addressing the presence of noise. Although statistical accuracy may appear high, such noise can distort area estimations for each class and lead to misinterpretation of the results. This presents a challenge when the output is intended to support decision-making processes.

Studies aimed at improving image quality have shown that majority filtering effectively removes salt-and-pepper noise in raster data (Olariu et al., 2022; Maleki et al., 2024). Salt-and-pepper noise typically appears as isolated pixels with values that differ from their neighbours, affecting both visual interpretation and quantitative analysis. Majority filtering tackles this by substituting the central pixel with the most common value among its surrounding pixels (Bayazit et al., 2025). This process helps to reduce local anomalies without significantly distorting the image structure. Applying this technique to the outputs of pixel-based classification can improve the accuracy and overall quality of land cover data generated using machine learning algorithms.

Sukajaya District, located in Bogor Regency, holds strategic importance within a conservation area due to its position in a mountainous region. Research by Tjahjono et al., (2024) indicates that Sukajaya District is highly prone to landslides. The local government has implemented ecologically oriented strategies to preserve the environmental quality of the area. Land cover mapping is crucial for generating accurate data to support environmentally based policy decisions. To effectively and efficiently detect detailed land cover features using open-source data, Sentinel-2 imagery with a 10 m resolution is well-suited for classification purposes. This study aims to enhance the quality of pixel-based RF land cover classification in Sukajaya District. To achieve high classification accuracy while minimising salt-and-pepper noise, the ntree was tuned and post-processing was applied using a majority filter to reduce noise and improve spatial coherence.

MATERIALS AND METHODS

Study Area

Sukajaya District is an administrative district within Bogor Regency, West Java Province (Fig. 1). Administratively, Sukajaya District shares borders with several districts in two regencies. To the west, it borders Cipanas and Lebakgedong Districts (Lebak Regency). To the south, it borders Cibeber District (Lebak Regency) and Nanggung District (Bogor Regency). To the east, it borders Nanggung and Cigudeg Districts (Bogor Regency). To the north, it borders Jasinga District (Bogor Regency). Situated within the Halimun Mountains and characterised by intense human activities, land use in Sukajaya District has become increasingly fragmented across different land cover types. This situation has led to more noticeable landscape fragmentation between land cover classes (Pramesti et al., 2025). Sukajaya District's varied landscape makes it an ideal study area for evaluating the performance of the RF classification algorithm and the use of majority filtering to improve land cover map accuracy. This is crucial for supporting spatial planning.

Materials

The administrative boundary of Sukajaya District was obtained from the Ina-Geoportal website. Sentinel-2 imagery from the year 2024 was used for land cover classification. Harmonised surface reflectance data from Sentinel-2 were retrieved via Google Earth Engine (GEE) and cloud masking was applied to remove contaminated pixels. To further reduce residual artefacts and temporal inconsistencies, a median filter was applied. All bands used in the analysis were resampled to a spatial resolution of 10 m using the nearest neighbour method, which preserves

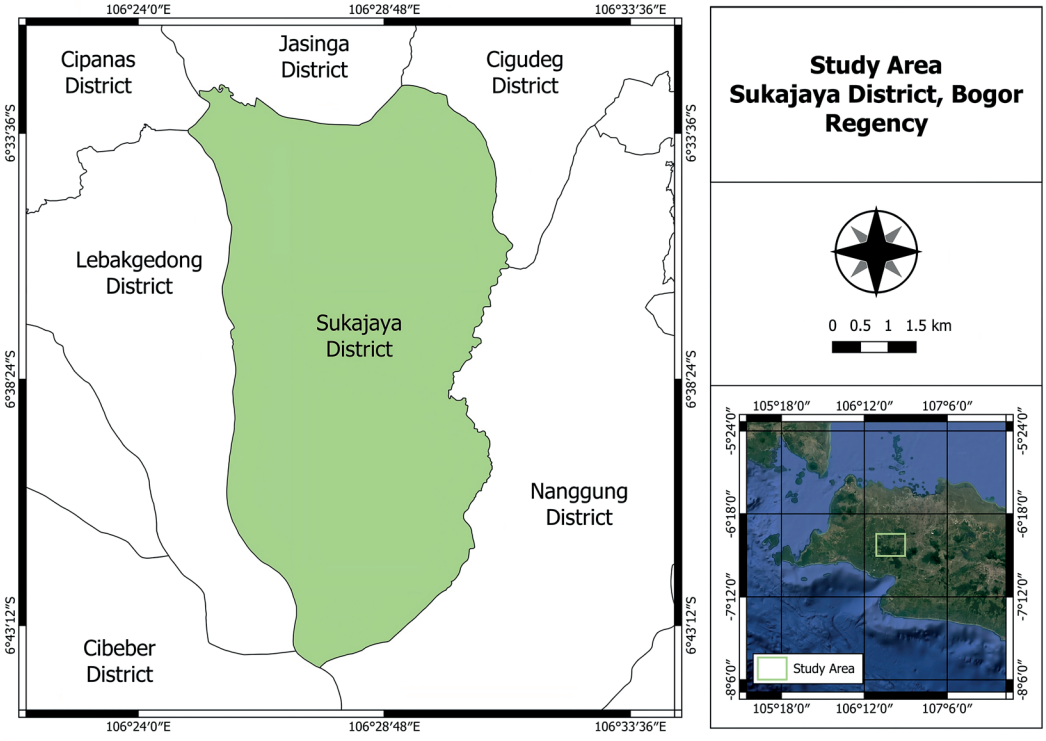

Fig. 1. The Map of Sukajaya District

original pixel values without introducing interpolation, thereby maintaining the integrity of the reflectance data. The specific Sentinel-2 bands used in the classification are listed in Table 1.

Land cover classes were defined following field surveys conducted in Sukajaya District. The classes and the number of datasets per class are presented in Table 2. The dataset consists of points derived from field verification and interpretation using Google Earth. This dataset was split using a 70/30 ratio, with 70 percent used as training data and 30 percent as validation data, following common practice in machine learning applications (Joseph, 2022). Consistently, the training data were used for land cover classification using the RF algorithm, with the ntree increasing incrementally from 100 to 700 in steps of 100. The validation data were used to assess the classification accuracy of both the RF results and the outputs after majority filtering in the post-processing stage.

Methods

Random Forest for Land Cover Classification

Random Forest (RF) is a supervised machine learning algorithm that works by building multiple decision trees in parallel during training, a technique called ensemble learning. The algorithm then combines the voting results from each tree to produce a more stable final decision (Breiman, 2001). The RF algorithm was implemented using GEE, which uses the Statistical Machine Intelligence and Learning Engine (SMILE) library as its backend. The SMILE RF library allows for efficient large-scale processing of geospatial data (Aji et al., 2024). This efficiency is achieved through direct integration with GEE's geospatial datasets and its support for parallel training. The number of trees (ntree) was tuned from 100 to 700 in steps of 100. With 10 Sentinel-2 bands, the number of variables per split was set to three, following the default setting of the square root of the input features.

Majority Filtering

Majority filtering is an image processing method used to reduce salt-and-pepper noise. It replaces the value of a central pixel with the majority value of its neighbouring pixels (S. Liu and Gu, 2017). Majority filtering was applied using the Sieve feature in QGIS to improve the land cover classification results from RF. This process uses an 8-neighbour rule (Ávila-Mosqueda et al., 2025), which considers all adjacent neighbouring pixels to determine the majority value for the central pixel. The majority filter assigns a pixel value based on the dominant value among its neighbouring pixels (Svoboda et al., 2022; Al-Aarajy et al., 2024). Mathematically, the original raster R consists of pixel values *R(i,j)*, where *i* and *j* represent the pixel coordinates. For each pixel (*i,j*), a local window *N(i,j)* is defined, which includes neighbours within a certain radius. The new pixel value *R'(i,j)* is calculated by taking the mode of *N(i,j)*, as shown in Equation 1:

$$R'(i,j) = mode(N(i,j)) \quad (1)$$

Here, *R'(i,j)* is the new pixel value obtained after applying majority filtering, and mode*(N(i,j))* is the most frequent value within the local window *N(i,j)*.

Table 1. Sentinel-2 bands used

Band	Description	Wavelength (nm)	Resolution (m)	Resample Resolution Used (m)
B2	Blue	490	10	10
B3	Green	560	10	10
B4	Red	665	10	10
B5	Red Edge 1	705	20	10
B6	Red Edge 2	740	20	10
B7	Red Edge 3	783	20	10
B8	Near Infrared (NIR)	842	10	10
B8A	Narrow NIR	865	20	10
B11	Short Wave Infrared 1	1610	20	10
B12	Short Wave Infrared 2	2190	20	10

Table 2. The amount of training and validation data collected for each land cover class

Land cover class	Data training amount	Data validation amount
Water body	405	173
Forest	401	172
Mixed garden	407	174
Oil palm plantation	412	177
Rice field	401	172
Bare land	169	72
Built-up area	403	173

Land Cover Class-based Accuracy Assessment

The classification results of the Random Forest model for each tested tree number, both without and with majority filtering, were evaluated based on accuracy per land cover class. The commonly used accuracy metrics in land cover classification are User's Accuracy (UA) and Producer's Accuracy (PA). UA represents the probability that a classified label is correct. This means it shows how accurately the pixels classified into a certain class truly belong to that class in the validation data. The formula for UA is presented in Equation 2.

$$UA_c = TP_c / \left(TP_c + FP_c \right) \quad (2)$$

PA indicates the classifier's ability to correctly identify pixels belonging to a specific class. It measures how many pixels from the actual class are correctly classified. The formula for PA is presented in Eq. 3.

$$PA_c = TP_c / \left(TP_c + FN_c \right) \quad (3)$$

When the number of validation samples is unbalanced across classes, it is recommended to use the F1-Score as an additional metric. This is because the F1-Score combines UA and PA into a single harmonic metric (Amin et al., 2024). The dataset sizes between subsets are unbalanced, resulting in unequal validation data for each land cover class. Therefore, in addition to calculating UA and PA, this research also uses the F1-Score metric. The formula for calculating the F1-Score is presented in Eq. 4.

$$F1_c = \left(2 \times UA_c \times PA_c \right) / \left(UA_c + PA_c \right) \quad (4)$$

Here, $F1_C$ is the F1-score for class c, UA_C is the user's accuracy for class c, PA_C is the producer's accuracy for the land cover class c, TP_C is the number of pixels correctly classified as class c, FP_C is the number of pixels incorrectly classified as class c but actually belong to other classes, and FN_C is the number of pixels that belong to class c but were misclassified as other classes.

Comprehensive Accuracy Assessment

The accuracy of the RF classification results, including tree number tuning and majority filtering, was assessed using Overall Accuracy (OA) and the Kappa Coefficient (KC). OA represents the percentage of total pixels or samples that were correctly classified when compared to the validation data. The formula for calculating OA is presented in Eq. 5.

$$OA = \sum_{i=1}^{K} TP_i / N \quad (5)$$

TP_i is the number of pixels correctly classified as class i. K is the total number of land cover classes. N is the total number of validation pixels across all classes.

Kappa coefficient (KC) is a statistical metric that measures the level of agreement between classification results and reference data, after correcting for the possibility of chance agreement. In short, KC accounts for the probability that a classification was correct purely by chance. The formula for calculating KC is presented in Equation 6.

$$k = \left(P_o - P_e \right) / \left(1 - P_e \right) \quad (6)$$

P_o is the number of correctly classified pixels divided by the total number of validation pixels, and P_e is derived from the product of the marginal totals in the classification and reference data.

RESULTS

Land Cover Raster from Random Forest with and without Majority Filtering

Pixel-based RF classification was conducted for each tested ntree without a majority filter. The results are illustrated in Fig. 2, and the corresponding land cover areas are presented in Fig. 3. The resulting land cover maps show variations in area depending on the ntree applied.

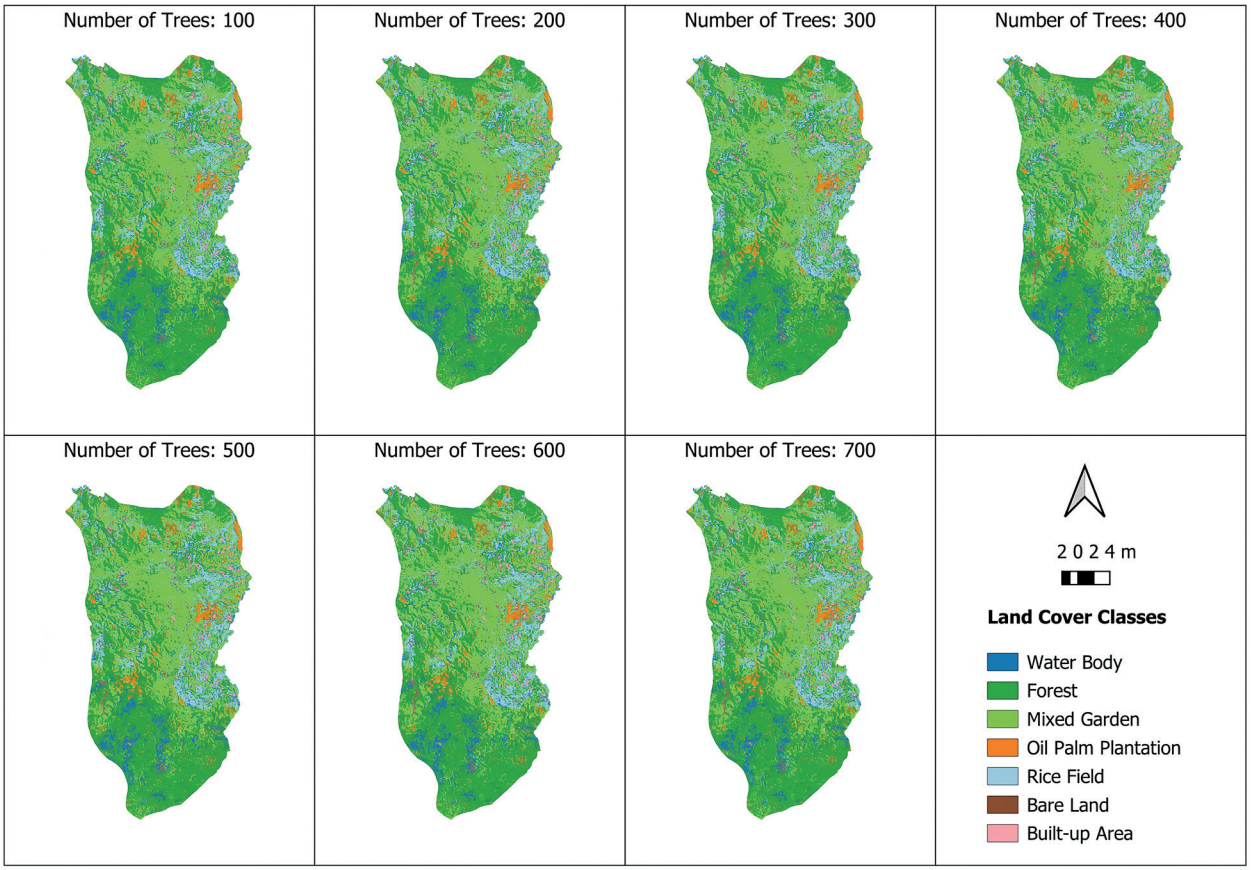

Fig. 2. Land cover classification using Random Forest without majority filter post-processing

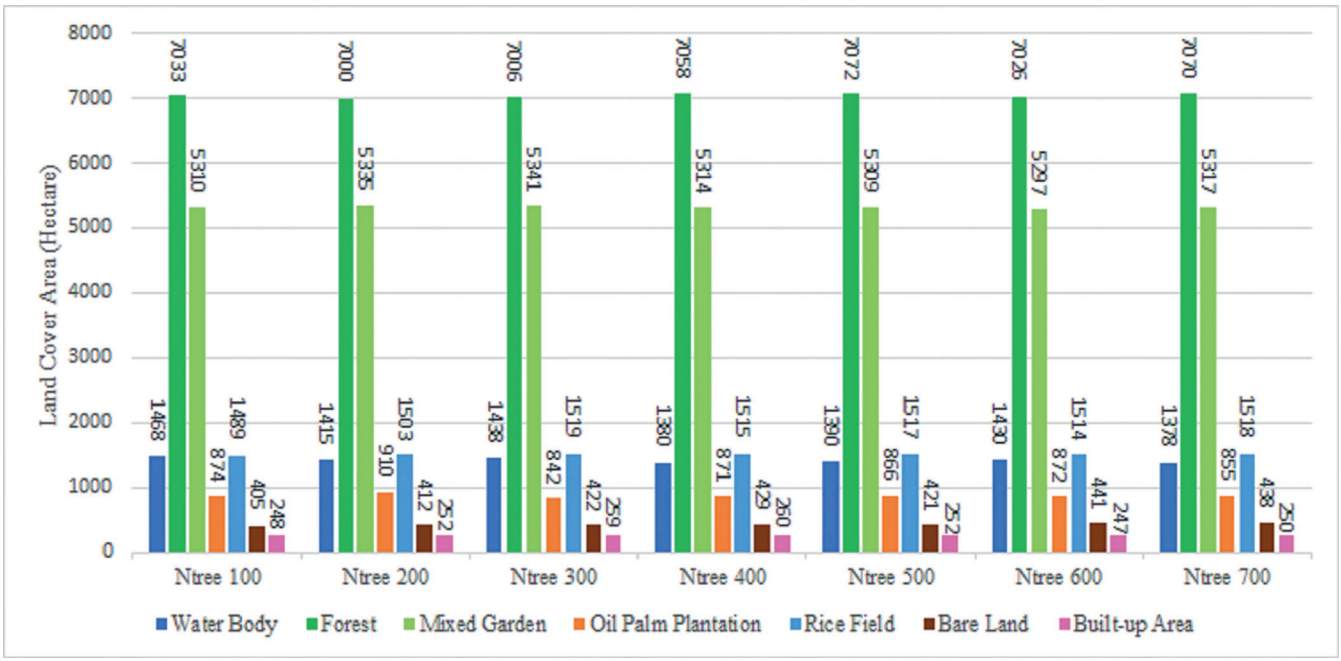

Fig. 3. Land cover class area from Random Forest classification without majority filter post-processing

Consistently, forest appeared as the dominant land cover, ranging from 7,000 to 7,070 ha. This was followed by mixed garden (5,297 to 5,341 ha), rice field (1,489 to 1,503 ha), water body (1,378 to 1,468 ha), oil palm plantation (842 to 910 ha), and bare land (405 to 441 ha). The smallest land cover class was built-up area, ranging from 247 to 259 ha. Despite these results, the classification outputs still show salt-and-pepper noise. This is characterised by small, scattered pixels that differ from the dominant surrounding class. This limitation comes from the pixel-based classification approach. In this method, each pixel is treated independently without considering the spatial pattern around it. This reduces both the accuracy and the visual quality of the land cover raster data.

Through the application of a majority filter, these noise speckles can be replaced by aligning pixel values with the dominant surrounding class. The post-processing results of the majority filter are shown in Fig. 4, and the area of each land cover class is presented in Fig. 5. The filtered output displays the same ranking of land cover areas from largest to smallest as in the unfiltered classification. However, differences in area are observed following the application of the majority filter. Forest remains the dominant land cover, ranging from 7,243 to 7,303 ha, followed by mixed garden (5,540 to 5,598 ha), rice field (1,481 to 1,505 ha), water body (1,091 to 1,151 ha), oil palm plantation (695 to 754 ha), and bare land (360 to 399 ha). Built-up area continues to represent the smallest land cover class, with an area between 261 and 273 ha.

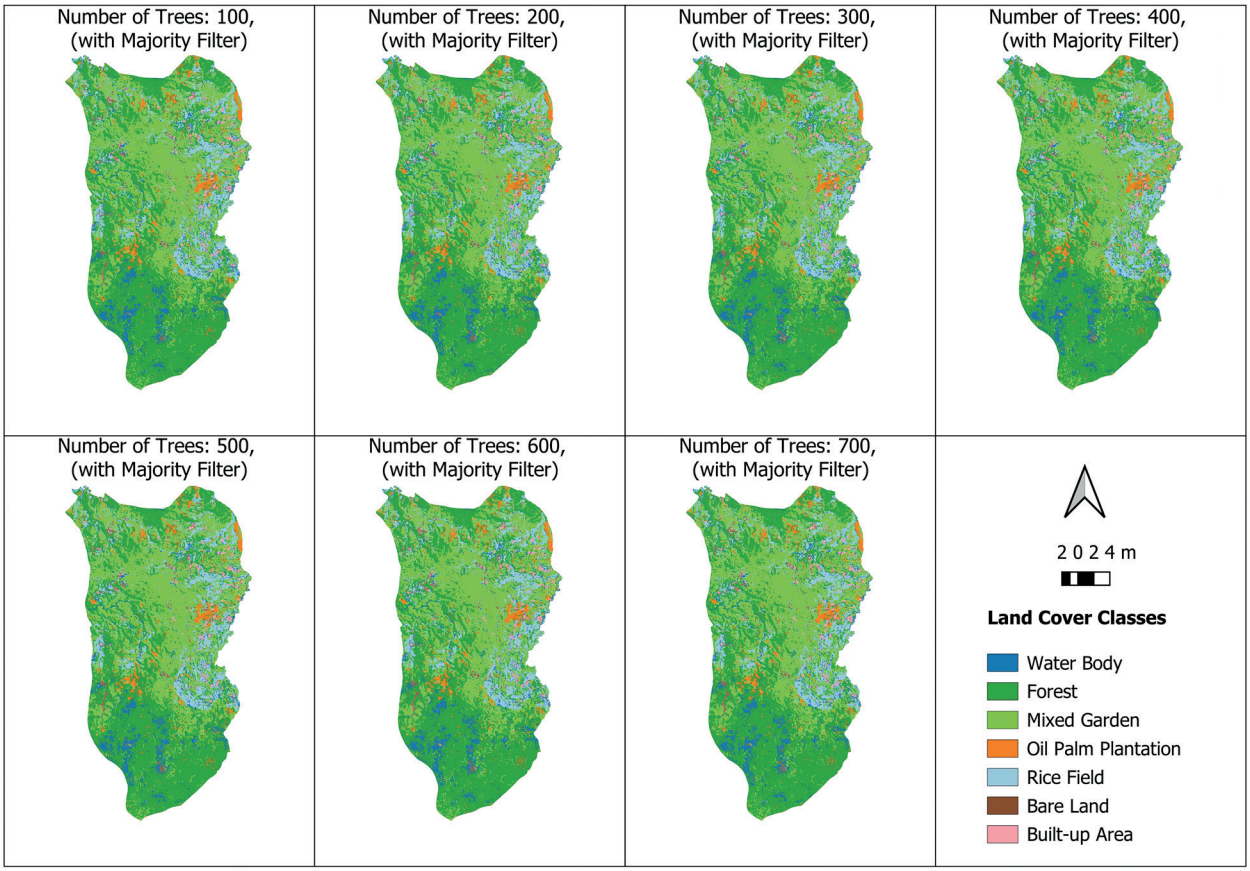

Fig. 4. Land cover classification using Random Forest with majority filter post-processing

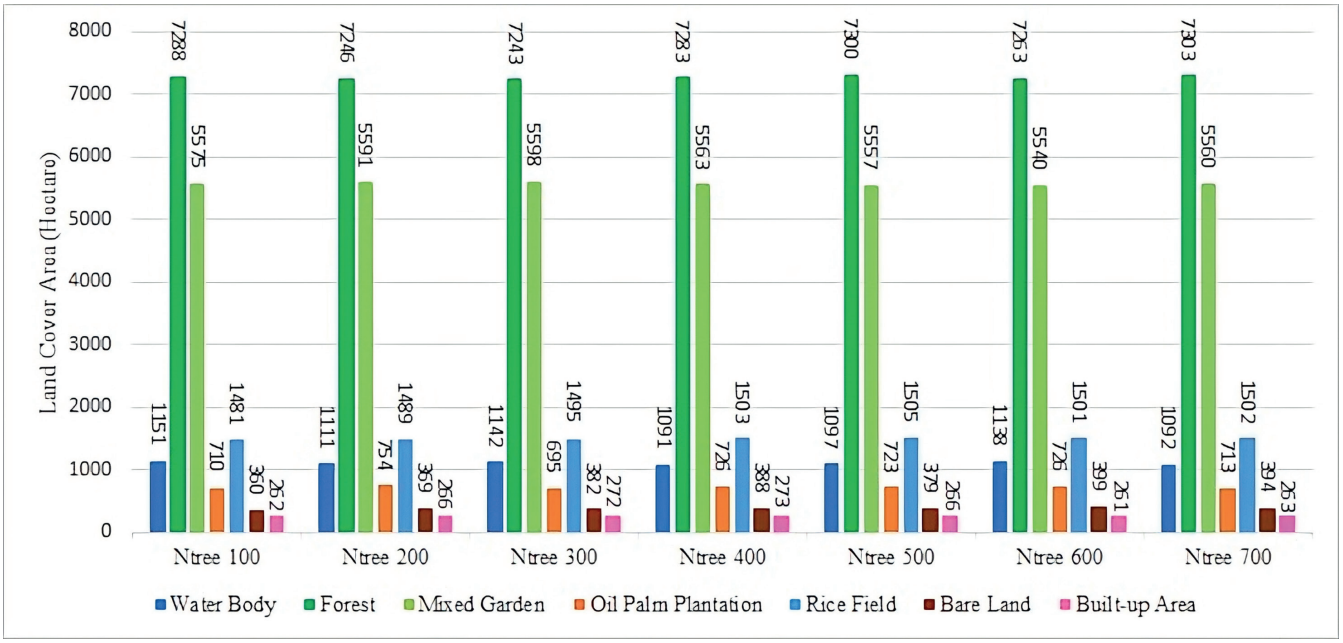

Fig. 5. Land cover class area from Random Forest classification with majority filter post-processing

A zoomed-in view is presented in Fig. 6 to illustrate in greater detail the differences between land cover classification results before and after applying the majority filter. The RF classification results using ntree values ranging from 100 to 700 without majority filtering display scattered speckles consisting of one to four pixels. These patterns give the impression of randomly distributed land cover patches with extremely small areas, approximately 100 to 400 m2. After applying the majority filter to each classification output across different ntree values, these speckles are eliminated. The majority filter works by reassigning pixel values to the most dominant land cover class within their neighbourhood, effectively transforming isolated pixels into more homogeneous clusters. As a result, small fragmented patches tend to shrink, while larger contiguous areas are expanded.

Accuracy of Land Cover Classification Per-Class with and without Majority Filtering

Visually, the majority filter enhances the quality of the land cover classification results. To better understand its impact on classification accuracy, an assessment was carried out for each land cover class. The classification accuracy per class was evaluated using User's Accuracy (UA) (Table 3), Producer's Accuracy (PA) (Table 4), and the F1-Score metric (Table 5).

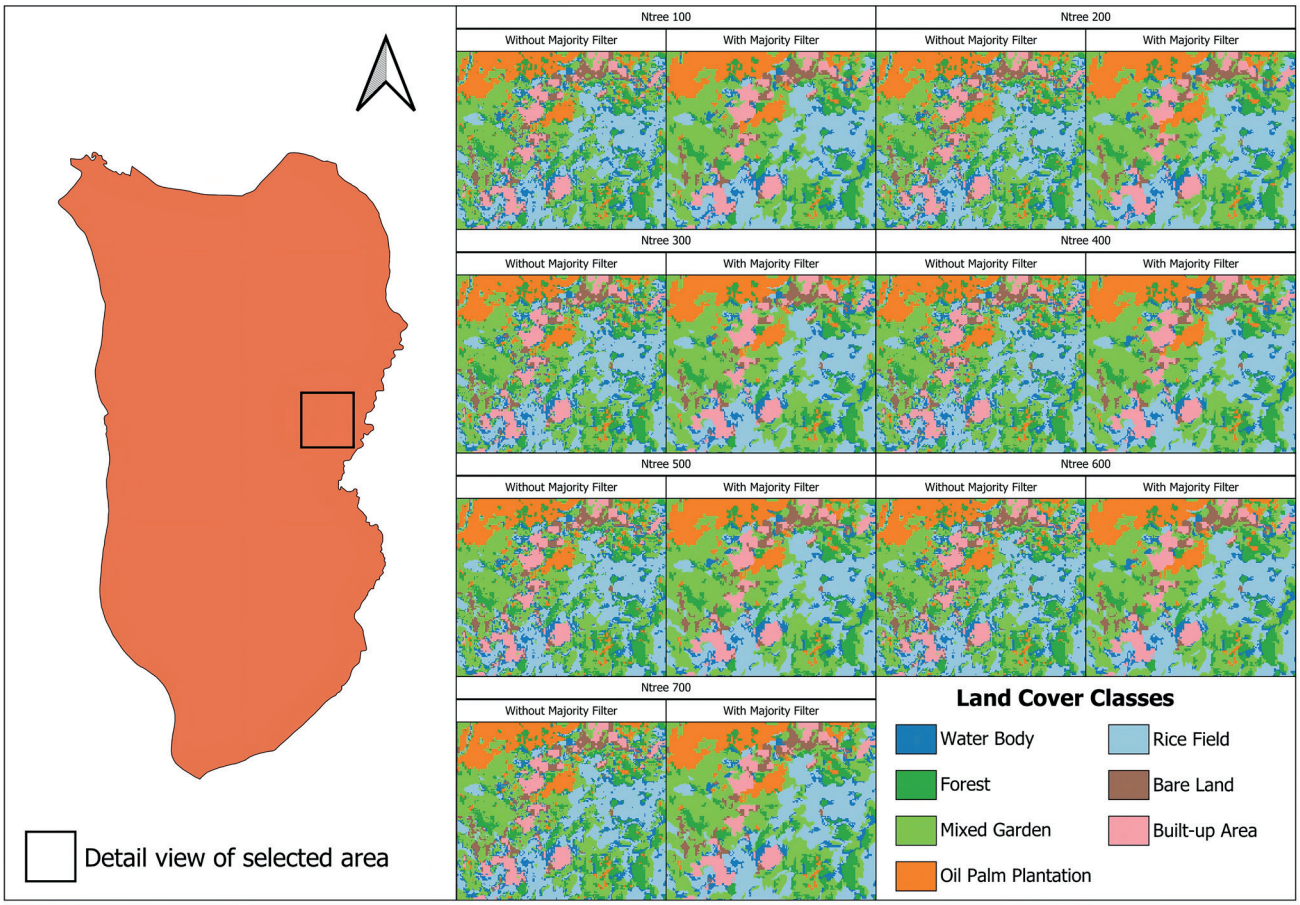

Fig. 6. Zoom-in comparison of land cover classification features using ntree 100–700 without and with majority filtering

The lowest accuracy values were observed for the bare land and water body classes. This can be attributed to the tropical wet conditions in Sukajaya District, where frequent rainfall causes bare land to become moist and appear non-homogeneous, complicating the classification process. This contrasts with bare land classifications in arid desert regions, which tend to be easier to classify (Darem et al., 2023; Du et al., 2023; Elmahdy and Mohamed, 2023). Similarly, water bodies in Sukajaya District are generally shallow, with partially exposed land and surrounding vegetation extending over the edges, resulting in high variability in conditions. This contributes to the reduced classification accuracy for this class. In contrast, other land cover classes that are relatively more homogeneous exhibit higher accuracy. Overall, classification accuracy is influenced by the degree of homogeneity within a land cover class; the more homogeneous the class, the higher its classification accuracy.

Based on UA values before and after applying the majority filter, accuracy shifts were generally positive, indicating that the majority filter improved the per-class accuracy of the land cover classification. This suggests a trend of increased accuracy in most land cover classes after the filter was applied, although variations in accuracy changes between classes were observed. Exceptions were found in the mixed garden class (except at ntree 200), bare land (ntree 400), and built-up area (ntree 400), which experienced decreases in accuracy. On average, the absolute change in UA reached 2.10 percentage points, showing that the majority filter had a measurable impact on classification accuracy. Based on PA values before and after the majority filter, only the bare land class showed a decline in accuracy, while the oil palm plantation class showed no improvements in accuracy. These results were consistent across ntree values from 100 to 700. The average absolute change in PA was calculated at 2.13 percentage points.

Based on F1-Score values before and after the application of the majority filter, the mixed garden class experienced a decrease in accuracy only at ntree 500. The bare land class showed an increase in accuracy only at ntree 600 and 700. Aside from these exceptions, a consistent improvement in accuracy was observed across ntree values from 100 to 700. The average absolute change was 1.88 points, reinforcing the finding that the filter tends to enhance the balance between UA and PA, despite slight variations in response across classes. Accuracy reductions in specific land cover classes based on UA, PA, and F1-Score metrics may occur when those classes are represented as small fragments. Although such fragments may have been correctly classified initially, the majority filter replaces them with the dominant surrounding class, thereby reducing the accuracy for those specific land cover categories.

Comprehensive Accuracy Assessment of Land Cover Classifications Before and After Majority Filtering

The comprehensive classification performance was evaluated using OA and KC, as shown in Fig. 7. In the first RF classification experiment with ntree set to 100, the map achieved a comprehensive accuracy with an OA of 81.94% and a KC of 78.72%. As the ntree value increased in increments of 100, the performance of the RF classifier improved, reaching its peak at ntree 400 for land cover classification. At this point, the model achieved an OA of 83.02% and a KC of 79.99%. Therefore, in this model, ntree 400 represents a plateau. A plateau refers to the stage where further increases in ntree do not result in additional performance gains (Probst and Boulesteix, 2018). When ntree was further increased in increments of 100, the accuracy exhibited diminishing returns. This indicates that after the RF model reaches its optimal accuracy, increasing the ntree may lead to a decline in performance. Similar results were also reported by Liu et al. (2021), who found that once the optimal ntree is reached, further increases in ntree can result in decreased performance.

Table 3. User's accuracy per land cover class from Random Forest classification (Ntree 100–700) without and with majority filtering

Method	User's Accuracy						
	Water Body	Forest	Mixed Garden	Oil Palm Plantation	Rice Field	Bare Land	Built-up Area
RF Ntree 100	67.20	78.60	75.90	94.50	81.30	67.90	99.40
RF Ntree 200	69.30	79.50	74.70	94.00	81.30	68.40	99.40
RF Ntree 300	69.80	80.70	75.60	95.60	81.50	70.20	99.40
RF Ntree 400	70.40	81.00	75.10	95.60	81.50	70.20	99.40
RF Ntree 500	70.40	79.70	75.40	96.10	82.80	66.10	99.40
RF Ntree 600	69.60	81.80	75.30	95.10	82.80	64.40	99.40
RF Ntree 700	70.00	80.80	75.10	94.50	82.40	65.00	99.40
RF Ntree 100 with Majority Filter	70.30	81.00	75.30	95.00	87.20	68.50	99.40
RF Ntree 200 with Majority Filter	72.90	80.90	75.30	95.10	86.50	69.80	99.40
RF Ntree 300 with Majority Filter	74.60	82.10	73.80	96.10	87.60	70.40	99.40
RF Ntree 400 with Majority Filter	75.90	82.30	75.00	97.70	83.70	68.50	98.80
RF Ntree 500 with Majority Filter	74.90	80.80	72.70	96.60	88.70	68.50	99.40
RF Ntree 600 with Majority Filter	72.80	82.80	74.40	96.70	87.60	68.50	99.40
RF Ntree 700 with Majority Filter	76.30	82.10	74.90	96.10	84.30	69.10	99.40

Table 4. Producer's Accuracy per land cover class from Random Forest classification (Ntree 100 – 700) without and with Majority Filtering

Method	Producer's Accuracy						
	Water Body	Forest	Mixed Garden	Oil Palm Plantation	Rice Field	Bare Land	Built-up Area
RF Ntree 100	71.10	79.10	74.10	97.20	86.00	52.80	96.00
RF Ntree 200	71.70	76.70	74.70	97.70	88.40	54.20	95.40
RF Ntree 300	73.40	77.90	74.70	97.70	89.50	55.60	95.40
RF Ntree 400	72.80	79.10	74.70	97.70	89.50	55.60	95.40
RF Ntree 500	72.80	79.70	74.10	97.70	89.50	54.20	95.40
RF Ntree 600	74.00	78.50	73.60	98.30	89.50	52.80	95.40
RF Ntree 700	72.80	78.50	73.00	97.70	90.10	54.20	95.40
RF Ntree 100 with Majority Filter	74.00	82.00	78.70	97.20	87.20	51.40	96.50
RF Ntree 200 with Majority Filter	74.60	81.40	78.70	97.70	89.50	51.40	96.50
RF Ntree 300 with Majority Filter	76.30	82.60	77.60	97.70	90.70	52.80	96.50
RF Ntree 400 with Majority Filter	76.30	83.70	77.60	97.70	89.50	51.40	96.50
RF Ntree 500 with Majority Filter	75.70	83.10	76.40	97.70	91.30	51.40	96.50
RF Ntree 600 with Majority Filter	77.50	81.40	77.00	98.30	90.70	51.40	96.50
RF Ntree 700 with Majority Filter	76.30	82.60	77.00	97.70	90.70	52.80	96.50

Table 5. F1-Score per land cover class from Random Forest classification (Ntree 100–700) without and with majority filtering

Method	F1-Score						
	Water Body	Forest	Mixed Garden	Oil Palm Plantation	Rice Field	Bare Land	Built-up Area
RF Ntree 100	69.10	78.80	75.00	95.80	83.60	59.40	97.60
RF Ntree 200	70.50	78.10	74.70	95.80	84.70	60.50	97.30
RF Ntree 300	71.50	79.30	75.10	96.60	85.30	62.00	97.30
RF Ntree 400	71.60	80.00	74.90	96.60	85.30	62.00	97.30
RF Ntree 500	71.60	79.70	74.80	96.90	86.00	59.50	97.30
RF Ntree 600	71.70	80.10	74.40	96.70	86.00	58.00	97.30
RF Ntree 700	71.40	79.60	74.10	96.10	86.10	59.10	97.30
RF Ntree 100 with Majority Filter	72.10	81.50	77.00	96.10	87.20	58.70	97.90
RF Ntree 200 with Majority Filter	73.70	81.20	77.00	96.40	88.00	59.20	97.90
RF Ntree 300 with Majority Filter	75.40	82.30	75.60	96.90	89.10	60.30	97.90
RF Ntree 400 with Majority Filter	76.10	83.00	76.30	97.70	86.50	58.70	97.70
RF Ntree 500 with Majority Filter	75.30	81.90	74.50	97.20	90.00	58.70	97.90
RF Ntree 600 with Majority Filter	75.10	82.10	75.70	97.50	89.10	58.70	97.90
RF Ntree 700 with Majority Filter	76.30	82.30	75.90	96.90	87.40	59.80	97.90

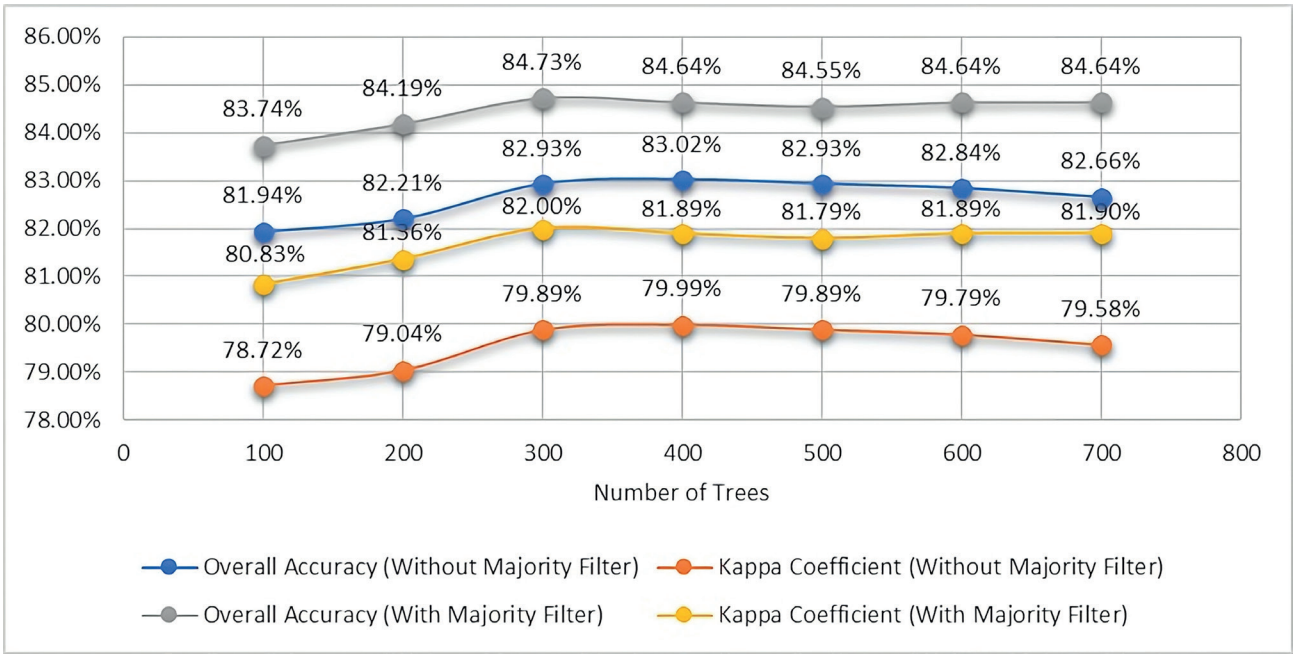

Fig. 7. Comprehensive accuracy of land cover classification using Random Forest (Ntree 100 – 700) with and without majority filter post-processing

After applying the majority filter, changes were observed in both OA and KC. Both metrics increased, confirming that post-classification processing with a majority filter can improve land cover classification quality by addressing salt-and-pepper noise. On average, OA increased by 1.80 percentage points, while KC saw a larger average improvement of 2.11 percentage points. However, this also led to a shift in the point of optimal accuracy. In the original classification results, the highest accuracy was achieved with an ntree value of 400. After majority filtering, the highest accuracy was instead observed with an ntree value of 300. Initially, the classification at ntree 400 had an OA of 83.02% and a KC of 79.99%, while ntree 300 had an OA of 82.93% and a KC of 79.89%. After the majority filter was applied, ntree 300 improved by 1.80 percentage points in OA and 2.11 percentage points in KC. In contrast, ntree 400 only improved by 1.62 percentage points in OA and 1.90 percentage points in KC. These findings confirm that the majority filter consistently enhances land cover classification quality. However, the extent of improvement does not directly correspond to the accuracy levels before post-processing. This is likely due to the inherent differences in classification outcomes produced by varying ntree settings, which lead to variations in the pixels most susceptible to reclassification during majority filtering.

Identical accuracy results were observed for ntree values of 400, 600, and 700 after applying the majority filter, despite their OA values being different before this filtering process. This indicates that although the initial classification results varied, the final outputs became identical after applying the majority filter, particularly in the areas used for validation. In other words, initial differences in classification had little impact on accuracy values because the majority filter produced uniform maps in the validation areas. However, a slight distinction remains in the KC values. The KC for ntree 400 and 600 remained the same after filtering, while the value for ntree 700 was slightly higher by 0.01 percentage points. This is due to the nature of the KC, which accounts for chance agreement. As a result, minor variations in classification patterns can still be detected, even when OA values are identical.

DISCUSSION

The study results indicate that majority filtering plays a vital role in enhancing the spatial coherence of land cover classification maps produced by RF by reducing salt-and-pepper noise. This finding aligns with the application of majority filtering demonstrated by Chen et al. (2023), where salt-and-pepper noise, consisting of minority pixels, is replaced by the majority class of neighbouring pixels. Although numerous studies have applied this technique and emphasised the advantages in reducing classification noise and enhancing spatial coherence, few have critically examined potential drawbacks. One notable yet often overlooked consequence is the removal of pixels that were correctly classified but belong to small, fragmented land cover patches. Such areas, despite being accurate representations of actual land cover, are susceptible to elimination due to excessively small spatial size. This effect is evident in the water body, oil palm plantation, rice field, and bare land classes, which consistently from ntree 100 to 700 experienced reductions in area after majority filtering. Conversely, land cover types characterised by larger fragment sizes such as forest, mixed garden, and built-up area consistently from ntree 100 to 700 showed increases in area.

Both the results with and without majority filtering consistently show that forest remains the dominant land cover in Sukajaya District, while built-up areas are the least extensive. Nevertheless, noticeable changes in area are clearly observed. The results after applying majority filtering are considered better, as the salt-and-pepper noise has been removed. Forest dominance is expected, as Sukajaya District, which spans from mountainous areas to the foothills, partly lies within a National Park forest area. Mountainous regions are often designated as protected zones, making forest cover the dominant class (Li et al., 2022). Findings from other highland regions consistently show that forest is the predominant land cover type (Adhikari et al., 2022; Ismail et al., 2021; Ratnayake et al., 2024). In the Himalayas, where permanent snow exists, forest is the second most dominant class after snow (Singh and Pandey, 2021). However, the presence of plantations or agricultural land as classes competing with forest for dominance is also frequently observed in areas that have

undergone deforestation. These differences largely depend on conservation policies and their enforcement, which shape human activities and the intensity of anthropogenic land use (Chen et al., 2025).

Through tuning the ntree, it was found that accuracy per land cover class generally improved, but some classes experienced a decline. The claim by Kuntla and Manjusree (2020) that majority filtering reduces commission errors and thus improves per-class accuracy cannot be fully accepted. This study demonstrates that, in the case of the bare land class, almost all ntree values tested showed decreases in both area and accuracy. This is because bare land is the most fragmented class, making it highly susceptible to negative externalities from majority filtering.

In studies using RF, tuning the ntree is typically performed to achieve high accuracy (Manafifard, 2024). Logically, the plateau point of ntree in RF is expected to yield higher accuracy than other ntree values, both before and after majority filtering. Although this has not been definitively proven, the present study suggests that accuracy can improve beyond the plateau point after post-classification majority filtering. The shift of maximum accuracy from ntree 400 (before filtering), which was considered the plateau in this experiment, to ntree 300 (after filtering) indicates that the relationship between the RF ntree tuning parameter and classification accuracy is not strictly linear when majority filtering is applied in post-processing. Even though ntree 400 initially produced the best overall accuracy, after majority filtering the best results shifted to ntree 300. This suggests that models with slightly lower initial performance may produce better results after majority filtering, depending on how the post-filtering changes align with the validation data locations.

It is important to emphasise that majority filtering is a post-classification procedure and does not affect the internal learning dynamics of the RF model. However, different ntree values can yield slightly different classification patterns (Sun and Ongsomwang, 2023). These differences influence the distribution of salt-and-pepper noise, which in turn determines the susceptibility of pixels to the majority filtering process. This phenomenon reflects the inherent randomness of the RF algorithm, arising from the bootstrapping process and random feature selection during tree construction, which ultimately affects the classification results (Salman et al., 2024). Consequently, although ntree 400 may produce the highest initial accuracy, the combination of noise distribution, filtering effects, and coincidentally more favourable variability at ntree 300 with slightly lower initial accuracy can lead to a more optimal improvement after majority filtering. Moreover, the accuracy difference between ntree 400 and ntree 300 prior to filtering is very small.

The phenomenon of identical OA values for ntree 400, 600, and 700 after filtering, despite different values before filtering, highlights the limitation of OA. OA only measures the proportion of correctly classified samples and does not account for agreement due to chance. In contrast, KC, which adjusts for random agreement, remains more sensitive in distinguishing model performance. This underscores the importance of using multiple accuracy metrics in land cover map evaluation. For this reason, land cover classification studies often employ both OA and KC as evaluation tools (Zeferino et al., 2020). These findings emphasise the importance of integrating pixel-based machine learning classification algorithms with spatial majority filtering techniques to support operational land cover mapping.

Majority filtering has proven effective in enhancing the spatial coherence of classification results and reducing noise. Therefore, studies that rely on pixel-based classification for purposes such as land cover change analysis (Kaur et al., 2023), urban expansion (Zhang et al., 2021), deforestation monitoring (Silva et al., 2022), estimating carbon stock changes (Wahyuni et al., 2025), soil erosion assessment (Belay and Mengistu, 2021), delineating geohazard-prone areas (Tempa and Aryal, 2022), and projecting land cover dynamics (Hakim et al., 2020) should apply majority filtering as a post-processing step to produce cleaner and more accurate results. Majority filtering also has the potential to remove small land cover patches that may have been correctly classified but are spatially vulnerable to being filtered out. This creates a trade-off between the visual accuracy gained from the positive effects of majority filtering and the preservation of spatial details that risk being lost due to its negative effects. Nevertheless, the overall benefits of applying majority filtering outweigh its side effects.

CONCLUSIONS

This study demonstrates that the RF algorithm can classify pixel-based land cover from Sentinel-2 imagery in Sukajaya District, Bogor Regency, with a performance plateau reached at ntree 400. However, the initial classification results still exhibit salt-and-pepper noise due to the inherent limitations of the pixel-based approach. The application of majority filtering improves land cover classification accuracy. This improvement allows performance to surpass that of the model with the best parameters before filtering, as evidenced by the accuracy of ntree 300 exceeding that of ntree 400 after filtering. Majority filtering affects land cover classes. Classes with large but fragmented patches tend to increase in size, whereas classes initially composed of small units tend to decrease. Overall, majority filtering effectively enhances the quality of classification results. It is recommended as a standard component in the workflow for pixel-based land cover classification. This supports evidence-based planning by offering an objective foundation for assessing environmental conditions.

REFERENCES

Adhikari J.N., Bhattarai B.P., Rokaya M.B. and Thapa T.B. (2022). Land use/land cover changes in the central part of the Chitwan Annapurna Landscape, Nepal. PeerJ, 10, e13435. DOI: 10.7717/peerj.13435

Aji A., Husna V.N. and Purnama S.M. (2024). Multi-Temporal data for land use change analysis using a machine learning approach (google earth engine). International Journal of Geoinformatics, 20(4), 19–28. DOI: 10.52939/ijg.v20i4.3145

Al-Aarajy K.H.A., Zaeen A.A. and Abood K.I. (2024). Supervised classification accuracy assessment using remote sensing and geographic information system. TEM Journal, 13(1), 396–403. DOI: 10.18421/TEM131-41

Altman N. and Krzywinski M. (2017). Ensemble methods: bagging and random forests. Nature Methods, 14(10), 933–934. DOI: 10.1038/nmeth.4438

Amin G., Imtiaz I., Haroon E., Saqib N. us, Shahzad M.I. and Nazeer M. (2024). Assessment of machine learning algorithms for land cover classification in a complex mountainous landscape. Journal of Geovisualization and Spatial Analysis, 8(34), 1–19. DOI: 10.1007/s41651-024-00195-z

Anthony T., Shohan A.A.A., Oludare A., Alsulamy S., Kafy A. Al and Khedher K.M. (2024). Spatial analysis of land cover changes for detecting environmental degradation and promoting sustainability. Kuwait Journal of Science, 51(100197). DOI: 10.1016/j.kjs.2024.100197

Aslam R.W., Shu H., Naz I., Quddoos A., Yaseen A., Gulshad K. and Alarifi S.S. (2024). Machine learning-based wetland vulnerability assessment in the Sindh Province Ramsar site using remote sensing data. Remote Sens., 16(928). DOI: 10.3390/rs16050928

Ávila-Mosqueda S.V., van Tussenbroek B.I. and Garza-Pérez J.R. (2025). Changes in seagrass landscape configuration in a Caribbean Reef Lagoon indicate an ecosystem shift after repeated disturbances. Coasts, 5(8). DOI: 10.3390/coasts5010008

Bayazit M., Dönmez C. and Berberoglu S. (2025). Assessing the efficiency of pixel-based and object-based image classification using deep learning in an agricultural Mediterranean plain. Environ. Monit. Assess., 197(155), 1–20. DOI: 10.1007/s10661-024-13431-2

Behera D.K., Pujar G.S., Kumar R. and Singh S.K. (2024). A comprehensive approach towards enhancing land use land cover classification through machine learning and object-based image analysis. Journal of the Indian Society of Remote Sensing, 53, 731–749. DOI: 10.1007/s12524-024-01997-w

Belay T. and Mengistu D.A. (2021). Impacts of land use/land cover and climate changes on soil erosion in Muga watershed, Upper Blue Nile basin (Abay), Ethiopia. Ecological Processes, 10(1). DOI: 10.1186/s13717-021-00339-9

Breiman L. (2001). Random forests. Machine Learning, 45, 5–32.

Chahal A., Gulia P., Gill N.S., Yahya M., Haq M.A., Aleisa M., Alenizi A., Khan A.A. and Shukla P.K. (2024). Predictive analytics technique based on hybrid sampling to manage unbalanced data in smart cities. Heliyon, 10(e39275). DOI: 10.1016/j.heliyon.2024.e39275

Chen J., Sasaki J., Guo Z. and Endo M. (2023). UAV-based seagrass wrack orthophotos classification for estimating blue carbon. Estuarine, Coastal and Shelf Science, 293. DOI: 10.1016/j.ecss.2023.108476

Chen W., Yuan Y., Gu T., Ma H. and Zeng J. (2025). What factors drove the global cropland expansion into highlands? Earth's Future, 13, e2024EF005337. DOI: 10.1029/2024EF005337

Darem A.A., Alhashmi A.A., Almadani A.M., Alanazi A.K. and Sutantra G.A. (2023). Development of a map for land use and land cover classification of the Northern Border Region using remote sensing and GIS. Egyptian Journal of Remote Sensing and Space Science, 26(2), 341–350. DOI: 10.1016/j.ejrs.2023.04.005

Du H., Li M., Xu Y. and Zhou C. (2023). An ensemble learning approach for land use/land cover classification of arid regions for climate simulation: A case study of Xinjiang, Northwest China. IEEE Journal of Selected Topics in Applied Earth Observations and Remote Sensing, 16, 2413–2426. DOI: 10.1109/JSTARS.2023.3247624

Ebrahimy H., Mirbagheri B., Matkan A.A. and Azadbakht M. (2021). Per-pixel land cover accuracy prediction: A random forest-based method with limited reference sample data. ISPRS Journal of Photogrammetry and Remote Sensing, 172, 17–27. DOI: 10.1016/j.isprsjprs.2020.11.024

Edosa B.T. and Erena M.G. (2024). Wildlife habitat suitability analysis and mapping the former dhidhessa wildlife sanctuary using GIS-based analytical hierarchal process and weighted linear combination methods. Heliyon, 10(e33921). DOI: 10.1016/j.heliyon.2024.e33921

El-Deen Taha L.G. and Mandouh A.A. (2024). Assessment of Random Forest and Neural Network for improving land use/ land cover mapping from LIDAR data and RGB image: A case study of Magaga-El-Menia Governorate, Egypt. Geoplanning: Journal of Geomatics and Planning, 11(1), 17–30. DOI: 10.14710/geoplanning.11.1.17-30

Elmahdy S.I. and Mohamed M.M. (2023). Regional mapping and monitoring land use/land cover changes: a modified approach using an ensemble machine learning and multitemporal Landsat data. Geocarto International, 38(1). DOI: 10.1080/10106049.2023.2184500

Fu B., Wang Y., Campbell A., Li Y., Zhang B., Yin S., Xing Z. and Jin X. (2017). Comparison of object-based and pixel-based random forest algorithm for wetland vegetation mapping using high spatial resolution GF-1 and SAR data. Ecological Indicators, 73, 105–117. DOI: 10.1016/j.ecolind.2016.09.029

Hakim A.M.Y., Matsuoka M., Baja S., Rampisela D.A. and Arif S. (2020). Predicting land cover change in the Mamminasata area, Indonesia, to evaluate the spatial plan. ISPRS Int. J. Geo-Inf., 9(481). DOI: 10.3390/ijgi9080481

Ibrahim M. (2023). Evolution of random forest from decision tree and bagging: A bias-variance perspective. DUJASE, 7(1), 66–71. DOI: 10.3329/dujase.v7i1.62888

Ismail M.H., Aik D.H.J., Alias M.A., Muharam F.M. and Zaki P.H. (2021). Land Use/Land Cover (LULC) Changes in Cameron Highlands, Malaysia: Explore the Impact of the LULC Changes on Land Surface Temperature (LST) Using Remote Sensing. In: Climate Impacts on Sustainable Natural Resource Management , 279–301. wiley. DOI: 10.1002/9781119793403.ch14

Joseph V.R. (2022). Optimal ratio for data splitting. Stat. Anal. Data Min.: The ASA Data Sci. Journal, 15, 531–538. DOI: 10.1002/sam.11583

Kaur H., Tyagi S., Mehta M. and Singh D. (2023). Time series (2001/2002–2021) analysis of earth observation data using Google Earth Engine (GEE) for detecting changes in Land Use Land Cover (LULC) with specific reference to forest cover in East Godavari Region, Andhra Pradesh, India. J. Earth Syst. Sci., 132(86), 1–16. DOI: 10.1007/s12040-023-02099-w

Kuntla S.K. and Manjusree P. (2020). Development of an automated tool for delineation of flood footprints from SAR imagery for rapid disaster response: a case study. Journal of the Indian Society of Remote Sensing, 48(6), 935–944. DOI: 10.1007/s12524-020-01125-4

Li B. V, Jenkins C.N. and Xu W. (2022). Strategic protection of landslide vulnerable mountains for biodiversity conservation under land-cover and climate change impacts. PNAS, 19(2), e22113416118. DOI: 10.1073/pnas.2113416118/-/DCSupplemental

Liu D., Zhang X., Zheng T., Shi Q., Cui Y., Wang Y. and Liu L. (2021). Optimisation and evaluation of the random forest model in the efficacy prediction of chemoradiotherapy for advanced cervical cancer based on radiomics signature from high-resolution T2 weighted images. Archives of Gynecology and Obstetrics, 303, 811–820. DOI: 10.1007/s00404-020-05908-5

Liu S. and Gu G. (2017). Improving the impervious surface estimation from hyperspectral images using a spectral-spatial feature sparse representation and post-processing approach. Remote Sens., 9(456). DOI: 10.3390/rs9050456

Maleki R., Wu F., Oubara A., Fathollahi L. and Yang G. (2024). Refinement of cropland data layer with effective confidence layer interval and image filtering. Agriculture, 14(1285). DOI: 10.3390/agriculture14081285

Manafifard M. (2024). A new hyperparameter to random forest: application of remote sensing in yield prediction. Earth Science Informatics, 17(1), 63–73. DOI: 10.1007/s12145-023-01156-8

Mensah J.K., Ofosu E.A., Yidana S.M., Akpoti K. and Kabo-bah A.T. (2022). Integrated modeling of hydrological processes and groundwater recharge based on land use land cover, and climate changes: a systematic review. Environmental Advances, 8(100224). DOI: 10.1016/j.envadv.2022.100224

Olariu H.G., Malambo L., Popescu S.C., Virgil C. and Wilcox B.P. (2022). Woody plant encroachment: Evaluating methodologies for semiarid woody species classification from drone images. Remote Sens., 14(1665). DOI: 10.3390/rs14071665

Pramesti T.V., Rushayati S.B. and Prasetyo L.B. (2025). Evaluating ecosystem recovery on degraded lands restoration using satellite-based spatial indicators in Mount Halimun Salak National Park, Indonesia. Ecological Engineering & Environmental Technology, 26(8), 363–374. DOI: 10.12912/27197050/208417

Probst P. and Boulesteix A.-L. (2018). To tune or not to tune the number of trees in random forest. Journal of Machine Learning Research, 18, 1–18. http://jmlr.org/papers/v18/17-269.html.

Qacami M., Khattabi A., Lahssini S., Rifai N. and Meliho M. (2023). Land-cover/land-use change dynamics modeling based on land change modeler. Annals of Regional Science, 70, 237–258. DOI: 10.1007/s00168-022-01169-z

Ratnayake S.S., Reid M., Larder N., Hunter D., Ranagalage M., Kogo B., Dharmasena P.B. and Kariyawasam C.S. (2024). Knowing the lay of the land: changes to land use and cover and landscape pattern in village tank cascade systems of Sri Lanka. Frontiers in Environmental Science, 12, 1353459. DOI: 10.3389/fenvs.2024.1353459

Rivai F.A., Asy'ari R., Fadhil M.H., Jouhary N.A., Saenal N., Ardan F., Pohan A., Pramulya R. and Setiawan Y. (2023). Analysis of land use and land cover changes using random forest through Google Earth Engine in Depok City. SSRS Journal B: Spatial Research, 1, 1–12.

Salman H.A., Kalakech A. and Steiti A. (2024). Random forest algorithm overview. Babylonian Journal of Machine Learning, 2024, 69–79. DOI: 10.58496/bjml/2024/007

Silva C.A., Guerrisi G., Del Frate F. and Sano E.E. (2022). Near-real time deforestation detection in the Brazilian Amazon with Sentinel-1 and neural networks. European Journal of Remote Sensing, 55(1), 129–149. DOI: 10.1080/22797254.2021.2025154

Singh G. and Pandey A. (2021). Evaluation of classification algorithms for land use land cover mapping in the snow-fed Alaknanda River Basin of the Northwest Himalayan Region. Applied Geomatics, 13(4), 863–875. DOI: 10.1007/s12518-021-00401-3

Solomon N., Pabi O., Annang T., Asante I.K. and Birhane E. (2018). The effects of land cover change on carbon stock dynamics in a dry Afromontane forest in northern Ethiopia. Carbon Balance and Manage., 13(14), 1–13. DOI: 10.1186/s13021-018-0103-7

Sun J. and Ongsomwang S. (2023). Optimal parameters of random forest for land cover classification with suitable data type and dataset on Google Earth Engine. Frontiers in Earth Science, 11, 1188093. DOI: 10.3389/feart.2023.1188093

Svoboda J., Štych P., Laštovička J., Paluba D. and Kobliuk N. (2022). Random Forest classification of Land Use, Land-Use Change and Forestry (LULUCF) using Sentinel-2 data—A case study of Czechia. Remote Sensing, 14(5). DOI: 10.3390/rs14051189

Tempa K. and Aryal K.R. (2022). Semi-automatic classification for rapid delineation of the geohazard-prone areas using Sentinel-2 satellite imagery. SN Applied Sciences, 4(5). DOI: 10.1007/s42452-022-05028-6

Tjahjono B., Firdania I. and Trisasongko B.H. (2024). Modeling landslide hazard using machine learning: a case study of Bogor, Indonesia. Journal of Natural Resources and Environmental Management, 14(2), 407–414. DOI: 10.29244/jpsl.14.2.407

Wahyuni N.I., Soemarno and Hasyim A.W. (2025). Estimating carbondioxide emission and mitigation strategies from land use and land cover change in Banyuwangi. J-PAL, 16(1), 9–14. DOI: 10.21776/ub.jpal.2025.016.01.02

Ye Z., Yang K., Lin Y., Guo S., Sun Y., Chen X., Lai R. and Zhang H. (2023). A comparison between Pixel-based deep learning and Object-based image analysis (OBIA) for individual detection of cabbage plants based on UAV Visible-light images. Computers and Electronics in Agriculture, 209. DOI: 10.1016/j.compag.2023.107822

Zeferino L.B., Souza L.F.T. de, Amaral C.H. do, Fernandes Filho E.I. and Oliveira T.S. de. (2020). Does environmental data increase the accuracy of land use and land cover classification? International Journal of Applied Earth Observation and Geoinformation, 91. DOI: 10.1016/j.jag.2020.102128

Zhang X., Estoque R.C., Murayama Y. and Ranagalage M. (2021). Capturing urban heat island formation in a subtropical city of China based on Landsat images: implications for sustainable urban development. Environmental Monitoring and Assessment, 193(3). DOI: 10.1007/s10661-021-08890-w

Zhu L., Xing H. and Hou D. (2022). Analysis of carbon emissions from land cover change during 2000 to 2020 in Shandong Province, China. Scientific Reports, 12(1). DOI: 10.1038/s41598-022-12080-0